Sensitivity improvement of dual-comb spectroscopy using mode-filtering technique

doi: 10.1364/OE.25.031730

Research Article | Vol. 25, No. 25 | 11 Dec 2017 | OPTICS EXPRESS 31730
Optics EXPRESS

Sensitivity improvement of dual-comb spectroscopy using mode-filtering technique

AKIKO NISHIYAMA,[1,2,3] SATORU YOSHIDA,[1,2] TAKUYA HARIKI,[1,2] YOSHIAKI NAKAJIMA,[1,2] AND KAORU MINOSHIMA[1,2,*]

[1]*Department of Engineering Science, Graduate School of Informatics, University of Electro-Communications (UEC), 1-5-1 Chofugaoka, Chofu, Tokyo 182-8585, Japan*
[2]*Japan Science and Technology Agency (JST), ERATO MINOSHIMA Intelligent Optical Synthesizer (IOS) Project, 1-5-1 Chofugaoka, Chofu, Tokyo 182-8585, Japan*
[3]*Research Fellow of the Japan Society for the Promotion of Science (JSPS), 1-5-1 Chofugaoka, Chofu, Tokyo 182-8585, Japan*
**k.minoshima@uec.ac.jp*

Abstract: In this study, we demonstrated an improvement in the detection sensitivity of dual-comb spectroscopy using the repetition rate multiplication of optical frequency combs. We compared the dual-comb signals in three dual-comb setups consisting of combinations of two combs with and without mode-filtering, and investigated how the repetition rate influences the signal-to-noise ratio (SNR) of dual-comb measurements. The dual-comb setups using high-repetition-rate combs enabled the absorption lines of HCN gas to be measured with a high SNR in a short averaging time, and real-time spectral data acquisition was realized using a low-sensitivity and low-resolution RF spectrum analyzer.

OCIS codes: (300.6300) Spectroscopy, Fourier transforms; (140.4050) Mode-locked lasers; (070.2615) Frequency filtering.

References and links

1. S. Okubo, K. Iwakuni, H. Inaba, K. Hosaka, A. Onae, H. Sasada, and F.-L. Hong, "Ultra-broadband dual-comb spectroscopy across 1.0–1.9 μm," Appl. Phys. Express **8**, 082402 (2015).
2. A. Nishiyama, S. Yoshida, Y. Nakajima, H. Sasada, K. Nakagawa, A. Onae, and K. Minoshima, "Doppler-free dual-comb spectroscopy of Rb using optical-optical double resonance technique," Opt. Express **24**(22), 25894–25904 (2016).
3. G. B. Rieker, F. R. Giorgetta, W. C. Swann, J. Kofler, A. M. Zolot, L. C. Sinclair, E. Baumann, C. Cromer, G. Petron, C. Sweeney, P. P. Tans, I. Coddington, and N. R. Newbury, "Frequency-comb-based remote sensing of greenhouse gases over kilometer air paths," Optica **1**, 290–298 (2014).
4. T. Ideguchi, T. Nakamura, Y. Kobayashi, and K. Goda, "Kerr-lens mode-locked bidirectional dual-comb ring laser for broadband dual-comb spectroscopy," Optica **3**, 748 (2016).
5. A. Asahara, A. Nishiyama, S. Yoshida, K. I. Kondo, Y. Nakajima, and K. Minoshima, "Dual-comb spectroscopy for rapid characterization of complex optical properties of solids," Opt. Lett. **41**(21), 4971–4974 (2016).
6. O. E. Bonilla-Manrique, P. Martín-Mateos, B. Jerez, M. Ruiz-Llata, and P. Acedo, "High-resolution optical thickness measurement based on electro-optic dual-optical frequency comb sources," IEEE J. Sel. Top. Quantum Electron. **23**, 5300107 (2017).
7. A. Asahara and K. Minoshima, "Development of ultrafast time-resolved dual-comb spectroscopy," APL Photonics **2**, 041301 (2017).
8. T. Ideguchi, S. Holzner, B. Bernhardt, G. Guelachvili, N. Picqué, and T. W. Hänsch, "Coherent Raman spectro-imaging with laser frequency combs," Nature **502**(7471), 355–358 (2013).
9. I. Coddington, N. Newbury, and W. Swann, "Dual-comb spectroscopy," Optica **3**, 414–426 (2016).
10. I. Coddington, W. C. Swann, and N. R. Newbury, "Coherent linear optical sampling at 15 bits of resolution," Opt. Lett. **34**(14), 2153–2155 (2009).
11. J.-D. Deschênes, P. Giaccarri, and J. Genest, "Optical referencing technique with CW lasers as intermediate oscillators for continuous full delay range frequency comb interferometry," Opt. Express **18**(22), 23358–23370 (2010).
12. S. A. Diddams, M. Kirchner, T. Fortier, D. Braje, A. M. Weiner, and L. Hollberg, "Improved signal-to-noise ratio of 10 GHz microwave signals generated with a mode-filtered femtosecond laser frequency comb," Opt. Express **17**(5), 3331–3340 (2009).
13. K. J. Mohler, B. J. Bohn, M. Yan, G. Mélen, T. W. Hänsch, and N. Picqué, "Dual-comb coherent Raman spectroscopy with lasers of 1-GHz pulse repetition frequency," Opt. Lett. **42**(2), 318–321 (2017).

#307504 https://doi.org/10.1364/OE.25.031730
Journal © 2017 Received 19 Sep 2017; revised 3 Nov 2017; accepted 5 Nov 2017; published 6 Dec 2017

Optics EXPRESS

14. V. Durán, P. A. Andrekson, and V. Torres-Company, "Electro-optic dual-comb interferometry over 40 nm bandwidth," Opt. Lett. **41**(18), 4190–4193 (2016).
15. M.-G. Suh, Q.-F. Yang, K. Y. Yang, X. Yi, and K. J. Vahala, "Microresonator soliton dual-comb spectroscopy," Science **354**(6312), 600–603 (2016).
16. J. Chen, J. W. Sickler, P. Fendel, E. P. Ippen, F. X. Kärtner, T. Wilken, R. Holzwarth, and T. W. Hänsch, "Generation of low-timing-jitter femtosecond pulse trains with 2 GHz repetition rate via external repetition rate multiplication," Opt. Lett. **33**(9), 959–961 (2008).
17. Y. Nakajima, H. Inaba, K. Hosaka, K. Minoshima, A. Onae, M. Yasuda, T. Kohno, S. Kawato, T. Kobayashi, T. Katsuyama, and F.-L. Hong, "A multi-branch, fiber-based frequency comb with millihertz-level relative linewidths using an intra-cavity electro-optic modulator," Opt. Express **18**(2), 1667–1676 (2010).
18. M. S. Kirchner, D. A. Braje, T. M. Fortier, A. M. Weiner, L. Hollberg, and S. A. Diddams, "Generation of 20 GHz, sub-40 fs pulses at 960 nm via repetition-rate multiplication," Opt. Lett. **34**(7), 872–874 (2009).
19. N. R. Newbury, I. Coddington, and W. Swann, "Sensitivity of coherent dual-comb spectroscopy," Opt. Express **18**(8), 7929–7945 (2010).
20. S. Okubo, Y.-D. Hsieh, H. Inaba, A. Onae, M. Hashimoto, and T. Yasui, "Near-infrared broadband dual-frequency-comb spectroscopy with a resolution beyond the Fourier limit determined by the observation time window," Opt. Express **23**(26), 33184–33193 (2015).

1. Introduction

The dual-comb technique has proven to be a valuable tool for a variety of applications, such as precise spectroscopy [1,2], remote sensing [3], solid material characterization [4–6], ultrafast time-resolved measurement [7], and spectro-imaging [8]. Dual-comb spectroscopy is based on Fourier-transform spectroscopy using two optical frequency combs with slightly different repetition frequencies. The interferometry of two comb pulse trains can realize short acquisition times to obtain an interferogram without mechanically scanning the interferometers, and enables high-precision, high-resolution, and broadband measurements simultaneously. In dual-comb spectroscopy, the comb repetition frequencies (f_{rep}) determine the sampling clock rate and spectral sampling intervals. A Nyquist frequency limit is $f_{rep}/2$, and down conversion factor of optical to radio frequency is $f_{rep}/\Delta f_{rep}$, therefore, observable spectral bandwidth (BW) is expressed as $f_{rep}^2/2\Delta f_{rep}$. Here, Δf_{rep} represents the difference between the repetition frequencies of two combs, and it must choose to satisfy the condition $\Delta f_{rep} < f_{rep}^2/2BW$. In many previous studies, frequency combs with f_{rep} ~10–100 MHz were used and Δf_{rep} was set to the hertz to kilohertz range to measure the spectra over several THz bandwidth. The Δf_{rep} also determines the minimum acquisition rate, then the minimum acquisition time reaches the sub-millisecond to sub-second range. However, in practice, a certain amount of averaging time is necessary to achieve a sufficient signal-to-noise ratio (SNR) in the observed spectra, because the broadband spectra including many frequency elements are measured by a single photodetector. The dynamic range of the photodetectors and subsequent RF amplification limits the SNR per unit averaging time of dual-comb spectroscopy [9].

To efficiently use all the available comb powers, it is important to choose suitable detector according to the available peak power and use it below the saturation limit. The saturation behavior of photodetectors has been studied, and several methods have successfully reduced the saturation effects caused by comb pulse trains. For example, balanced detection schemes subtract the common DC input current [10], and furthermore chirped pulse methods reduce the pulse peak powers [11]. The use of high-repetition-rate combs also reduces the saturation effects caused by the reduction in pulse peak powers [12]. Recently, some groups demonstrated high-speed dual-comb measurements using high-repetition-rate combs with a f_{rep} higher than the gigahertz range [13–15]. In these applications, the high-repetition-rate combs enable high acquisition rates and high SNR measurements. Generating high-repetition-rate combs directly from mode-locked laser cavities generally requires a difficult alignment with limited stability. Moreover, it is difficult to generate octave-spanning spectra using nonlinear wavelength conversion, which is essential for comb stabilization by detecting the offset frequency (f_{ceo}) with a self-referencing scheme. In this work, we demonstrate the sensitivity enhancement of dual-comb spectroscopy by repetition rate multiplication with the

Optics EXPRESS

mode-filtering of the comb. We investigate in detail how the repetition rate influences the SNR of dual-comb spectroscopy. We develop a dual-comb system employing Er-fiber-based combs and the mode-filtering technique [12,16]. The use of the mode-filtering technique enables us to utilize fully stabilized low-repetition-rate combs and choose the feasible parameters of dual-comb spectroscopy for any application on demand, such as the measurement speed and sampling resolution.

2. Experimental setup for dual-comb spectroscopy using mode-filtered combs

2.1 Mode-filtering of an optical frequency comb

A schematic of the mode-filtering of an optical frequency comb using a Fabry–Perot cavity is illustrated in Fig. 1(a). We used a home-made Er-fiber comb with a f_{rep} of 56.6 MHz. The comb output was amplified and input to the Fabry–Perot cavity constructed from a pair of mirrors with a peak reflectivity of 0.99 at 1.5 μm, corresponding to a cavity finesse of 310. The cavity length was stabilized to overlap the cavity resonances with every 26th comb mode, and the free spectral range (FSR) of the cavity was then obtained to be 1.47 GHz. A part of the transmittance of the comb output was used to obtain the error signal that was fed back to a piezoelectric transducer (PZT) attached to one of the cavity mirrors. We employed a standard dither lock with a modulated frequency of 10 kHz. Figure 1(b) presents the amplified comb spectrum (black) and the transmitted comb spectrum (red) of the cavity. A sufficient coupling bandwidth is obtained because of the cavity finesse and low-dispersion mirrors [18]. Figure 1(c) presents the RF spectrum of the filtered comb. A multiplied repetition rate is observed and the side mode suppression ratio is 25.5 dB. After the mode-filtering, output power was lower than input power to the cavity because most of the non-resonant modes are reflected back to the input path. However, if we compare the mode powers in the same average power, filtered comb modes are larger than before filtering.

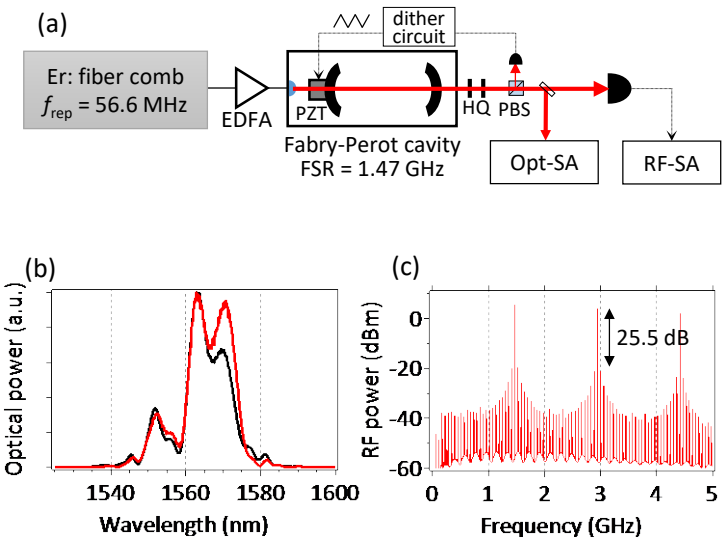

Fig. 1. (a) Schematic of the mode-filtering of an optical frequency comb. EDFA: Er-doped fiber amplifier, PZT: piezoelectric transducer, H: half-wave plate, Q: quarter-wave plate, Opt-SA: optical spectrum analyzer, RF-SA: RF spectrum analyzer. (b) Optical spectra before (black) and after (red) the Fabry–Perot cavity. (c) RF spectrum of the mode-filtered comb.

2.2 Setup for dual-comb spectroscopy

The experimental setups of the dual-comb spectroscopy are illustrated in Fig. 2. We used three types of setups: (a) without mode-filtering (Type 0), (b) one-comb filtering (Type 1), and (c) two-comb filtering (Type 2). In all three setups, the two outputs with equivalent

Optics EXPRESS

powers were overlapped and input to a photodetector (PD, New focus 1611). The phase-locking scheme of the dual-comb was based on [2]. One f_{rep} and the offset frequencies of two combs were phase-locked to the RF signals referencing a global-positioning-system-calibrated clock with an uncertainty of 3×10^{-12} over 1 s. Another f_{rep} was phase-locked to a continuous-wave (cw) laser at 1560 nm, and the cw laser was locked to an RF-stabilized comb mode. The comb f_{rep} and the cw laser frequency enable high-speed control by applying feedback to the intra-cavity electro-optical modulator [17] and injection current, respectively. A narrow relative linewidth between the two combs was achieved, and a relative linewidth below 1 Hz was maintained after the mode-filtering.

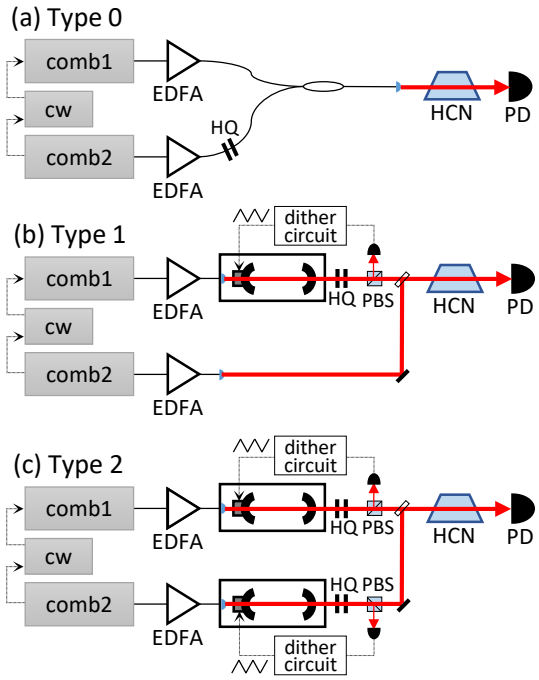

Fig. 2. Three dual-comb setups used in this study with a HCN cell as the sample: (a) Type 0, without filtering; (b) Type 1, one-comb filtering; (c) Type 2, two-comb filtering.

3. Experimental results

3.1 Heterodyne beats observed in each dual-comb setup

First, without the sample, heterodyne dual-comb beat notes are observed in each dual-comb setup. Figure 3 presents the beat spectra observed when Δf_{rep} was 100 Hz and the total input power to the photodetector was 10 μW. We used an RF spectrum analyzer (Rohde & Schwarz, FSW) with a resolution of 1 Hz to measure the fully resolved heterodyne beat notes. As shown in Fig. 3(a), in the dual-comb setup of Type 0, the mode spacing of the heterodyne beats is Δf_{rep} and the beats observed below the Nyquist frequency of $f_{rep}/2$. In the setup of Type 1 and Type 2 (Figs. 3(b) and 3(c), respectively), the beat notes with a mode spacing of $M \times \Delta f_{rep}$ were observed below the Nyquist frequencies of $f_{rep}/2$ and $M \times f_{rep}/2$, respectively. Here, M is the multiplication factor of the mode filtering, and it is 26 in this work. In the measurement of Type 2, we chose a suitable filtering comb mode to observe the beat note at the same frequency region as the other setups. The observed peak powers of the heterodyne beats are –121.1, –105.2, and –91.7 dBm in each setup. The residual side-modes of the filtered combs are separated in the frequency domain, so that they do not affect the main heterodyne beat signals. The mode-filtered combs with a multiplication factor of M have an

Optics EXPRESS

M-times-higher mode power than that before filtering in the case of the comparison at the same average power of the pulse trains. Therefore, the enhancement of the signal peak powers of the heterodyne beats in Type 1 and Type 2 from Type 0 is calculated to be M and M^2, respectively. The ratio of the observed peak powers agrees well with the estimations.

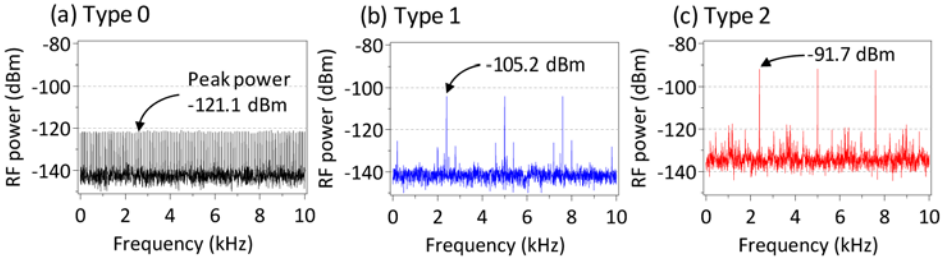

Fig. 3. Heterodyne beat spectra observed in each dual-comb setup without HCN cell: (a) Type 0, (b) Type 1, and (c) Type 2. In all the measurements, the input power to the detectors was 10 μW and the resolution of the RF spectrum analyzer was 1 Hz.

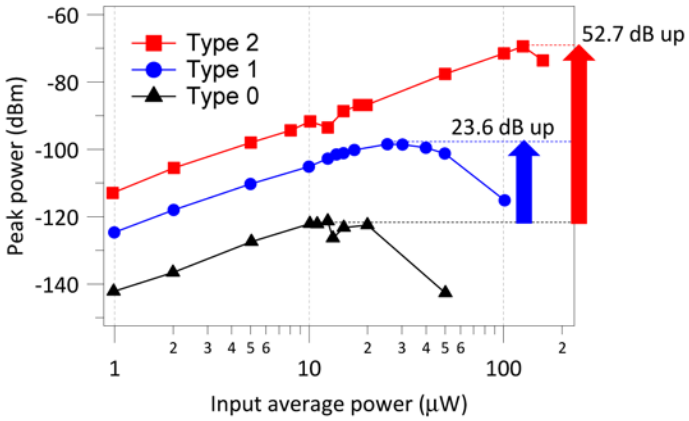

Fig. 4. RF peak power of the heterodyne beats observed in Type 0 (black), Type 1 (blue), and Type 2 (red) versus total input power to the photodetector.

The advantage of the repetition rate multiplication is not only the enhancement of the mode powers but also the reduction of the saturation effect of the photodetectors. The RF peak powers of the heterodyne beat notes are plotted in Fig. 4 versus the total input average power to the photodetector. As shown in Fig. 4, the reduction of the saturation effect is clearly observed. In the linear response region of the detector, RF peak powers are proportional to the square of input average power. The saturation of the detector is observed at 10 μW in the setup of Type 0, 25 μW in Type 1, and 125 μW in Type 2. By the combination of these two effects, a significant enhancement in the heterodyne beat peak powers of 23.6 and 52.7 dB in Type 1 and Type 2, respectively, are observed at the saturation input powers compared with Type 0. Table 1 presents the estimations and observed results of the ratio of the peak powers of the heterodyne beats, and they agree well with the results. The observed enhancement of the maximum peak powers at the saturation is slightly smaller than the estimation. This is because the saturation powers were slightly lower than the calculation, which could be caused by the difference in the chirps of the pulses in each setup, or the effect of the residual side modes of the mode-filtering.

Optics EXPRESS

Table 1. Ratio of the Peak Powers of the Dual-Comb Heterodyne Beat.

Setup	Calculation		Observations (dB)
		(dB)	
Type 1/Type 0 (10 μW)	M	14.1	15.9
Type 2/Type 0 (10 μW)	M^2	28.3	29.4
Type 1/Type 0 (saturation power)	M^2	28.3	23.6
Type 2/Type 0 (saturation power)	M^4	56.6	52.7

3.2 Absorption spectroscopy of HCN

We demonstrated the absorption spectroscopy in the setup of Type 0 and Type 1. In both cases, the input power to the detector was 10 μW and we used a 15-cm-long cell filled with 25 Torr of $H^{13}C^{14}N$ gas for the demonstration. Interferograms were obtained by a digitizer (NI PXIe-5122) with a sampling clock rate of f_{rep}. The maximum acquisition rate of the digitizer was 100 MHz, then we demonstrated only in the setup of Type 0 and Type1 because the Type2 setup needs 1.47 GHz sampling clock rate. The two stabilized comb frequencies satisfy the requirement for coherent averaging, and $f_{rep}/\Delta f_{rep}$ is an integer [10]. The Δf_{rep} was set to 100 Hz in this measurement. In addition, we employed phase correction software to coherently average the observed interferograms. Figures 5(a) and 5(b) show the $1/\Delta f_{rep}$ length of the interferogram and the magnified view of a center burst averaged over 2 s measured in Type 0 and Type 1, respectively. Figure 5(a) shows a single center burst in the total span. In Fig. 5(b), a multiplicative pulse train, which has 26 center bursts, is observed. The advantage of using the high-repetition comb in dual-comb measurement is short acquisition time of a interferogram, it is $1/26\Delta f_{rep}$ in this measurement. In other word, the high-repetition comb realizes averaging of multi interferograms in a period of $1/\Delta f_{rep}$. These pulse trains exhibit the same average power, but the pulse peak power decreases by the multiplication of the pulses.

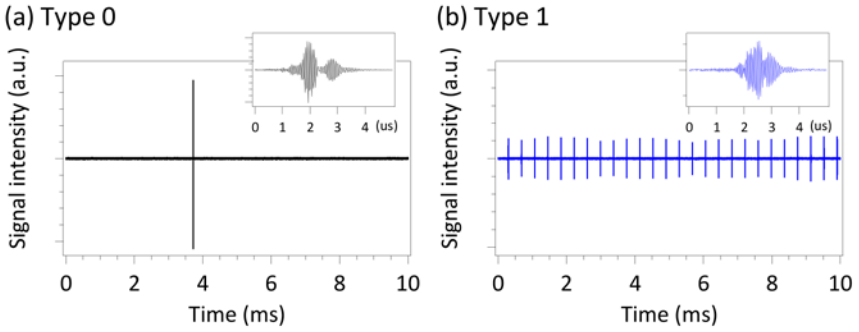

Fig. 5. Interferograms observed in the setup of (a) Type 0 and (b) Type 1. The insets show the magnified views around a center burst. The averaging time was 2 s.

Figure 6(a) presents the dual-comb spectra obtained from the Fourier transform of the interferograms of Fig. 5(a). The very noisy spectrum represented as a gray line was calculated from the unapodized interferogram, and the black line represents the apodized spectrum with a resolution of 1.47 GHz. Even after apodization, it is difficult to identify some HCN absorption lines. In contrast, Fig. 6(b) shows the mode-filtered comb spectrum. The spectrum was calculated from the interferogram of Fig. 5(b) including the 26 center bursts, and only the filtered comb modes are plotted. Although the profile shapes of the two spectra are different because of the filtering, the effect in the measured sensitivity is clearly shown. In the filtered dual-comb spectrum, absorption lines are clearly observed, and a significant sensitivity improvement by the mode-filtered comb is demonstrated.

Optics EXPRESS

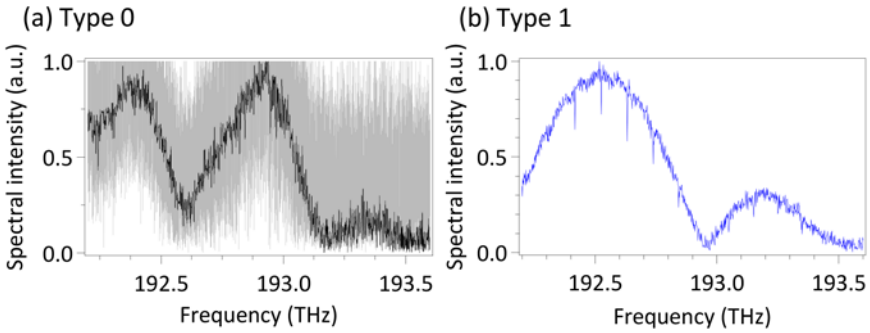

Fig. 6. Dual-comb spectra around HCN absorptions observed with same input power of 10 μW and same averaging time over 2 s. (a) Calculated spectra from unapodized (gray) and apodized (black) interferogram of Fig. 5(a). The apodized resolution was 1.47 GHz. (b) Mode-filtered comb spectrum calculated from the interferogram of Fig. 5(b) including the 26 center bursts.

3.3 Real-time measurement with RF spectrum analyzer

RF spectrum analyzers also enable a dual-comb heterodyne beat to be obtained directly, as demonstrated in Sec 3.1, which is attractive for practical applications. RF spectrum analyzers have basically two types of spectral acquisitions mode, FFT based acquisition mode and superheterodyne based sweep mode. In general, the RF spectrum analyzer with only the sweep mode is inexpensive but low sensitivity and low resolution than the FFT based spectral acquisitions. If the inexpensive spectrum analyzer can realize high-resolution real-time data acquisition of dual-comb signal, it is advantageous that the system become easy-to-use, convenient for carry and low cost. However, when we use the low-performance RF spectrum analyzers with a low sensitivity and low resolution, small heterodyne beat signals are buried in the large noise floor of the instruments, and dual-comb spectral resolution is limited by the resolution of spectrum analyzer. In the case that the resolution (δf_{RF}) of RF spectrum analyzer is larger than the mode spacing of dual-comb beats, the spectral resolution in optical region is expressed as $f_{rep}(\delta f_{RF}/\Delta f_{rep})$. In order to realize high-resolution measurement using low-resolution RF spectrum analyzer, the Δf_{rep} should be set to as large as possible. The dual-comb using mode-filtered combs enables us to use superheterodyne-based sweep mode RF spectrum analyzers because the heterodyne beats have high peak powers and Δf_{rep} can be set to larger values even for a wide measurement optical bandwidth, due to the mitigation of the limitation of observable optical spectral bandwidth which is $(Mf_{rep})^2/2M\Delta f_{rep}$.

The heterodyne beat spectrum of the transmittance of the HCN cell was measured in the setup of Type 2 by an RF spectrum analyzer with a resolution of 30 kHz and noise level of –110 dBm. The noise floor is higher than the peak power of dual-comb beat we observed with the setup of Type 0 (Fig. 3 (a)). The Δf_{rep} was 1 kHz, thus the mode spacing of the heterodyne beats was 26 kHz and observable optical spectral width was about 40 THz. In the setup of Type 0 and Type 1, the Δf_{rep} value of 1 kHz cannot accommodate the full comb spectral width because of the Nyquist limit, therefore even smaller Δf_{rep} is needed, and thus it degrades spectral resolution in optical domain as discussed above. Observed spectrum is presented in Fig. 7. The spectrum is obtained by a single sweep of the RF spectrum analyzer with a sweep time of 5.2 s. The lower horizontal axis shows frequency axis of RF spectrum analyzer, and upper one shows the optical frequency axis calculated from two comb frequencies. The measurement bandwidth in the RF domain was 10 MHz, and the observed bandwidth in the optical region was 570 GHz. In this measurement, the resolution of the RF spectrum analyzer was approximately set to the mode-spacing so that it can obtain a directly smooth absorption spectrum without comb mode structures, and thus observed spectrum includes averaged residual side mode powers. In the optical region, the resolution was calculated as 1.7 GHz. As shown in Fig. 7, the spectral resolution is enough to resolve sharp absorption structure of the

Optics EXPRESS

HCN gas. In addition, from the calibrated absolute optical frequency axis, these transitions are easily assigned as well-known transitions.

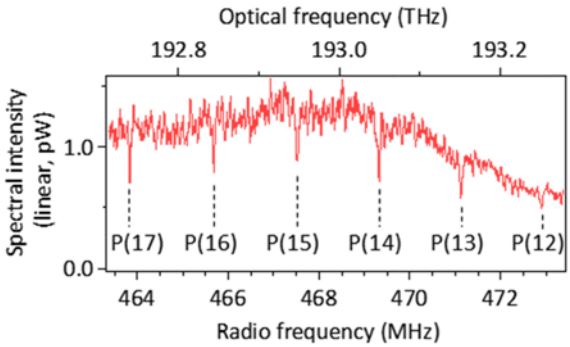

Fig. 7. Dual-comb heterodyne beat spectrum of the transmittance of the HCN cell measured by the low-resolution RF spectrum analyzer with a resolution of 30 kHz and acquisition time of 5.2 s. The assignments of the transitions are shown under the absorptions.

4. Discussion

Figure 8 shows the SNRs of the dual-comb heterodyne beats plotted as a function of input average power resulting from the same measurement shown in Fig. 4. By the mode-filtering of the comb, a clear enhancement in the SNRs of 19.9 and 23.6 dB in Type 1 and Type 2, respectively, relative to Type 0 are demonstrated. However, the SNR does not exhibit as significant an enhancement as that in Fig. 4. At low input powers (< 10 μW) in the setup of Type 0 and Type 1, the SNRs are proportional to the square of the input power because the limitation of the SNR is the detector noise. In contrast, in Type 2 and at high input power in Type 1, the SNRs reach the relative intensity noise (RIN) limit before the saturation limit [19]. The RIN limitation is shown around 40 dB. In this measurement, we speculate that the dominant intensity noise is caused by the mode-filtering scheme using dither lock. The fluctuations of the Fabry–Perot cavities and the modulations to obtain the error signals introduce intensity fluctuations in the comb transmissions. Thus, applying the other locking methods will further improve the SNR of the mode-filtered dual-comb heterodyne beats.

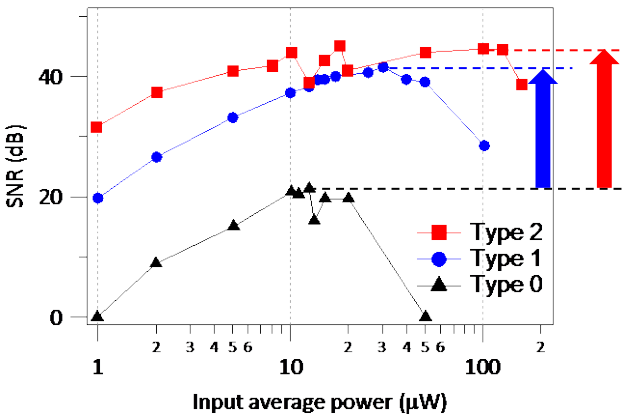

Fig. 8. SNR of the dual-comb heterodyne beats.

5. Conclusions

In this study, we achieved a significant improvement in sensitivity of dual-comb signals using mode-filtered optical frequency combs. The multiple-repetition-rate combs increased the RF

Optics EXPRESS

signal peak power up to 52.7 dB of the dual-comb heterodyne beat as a result of the enhancement of the mode powers and the reduction in the photodetector saturation effect. In the demonstration of absorption spectroscopy, the mode-filtered dual-comb (Type 1) achieved a high-SNR measurement of the HCN absorption signal in a short averaging time using a digitizer for the data acquisition. In addition, the setup of Type 2 realized real-time measurements of the HCN absorption spectra with single sweep mode of an RF spectrum analyzer with a low sensitivity and low resolution. The direct dual-comb measurement with the practical RF spectrum analyzer is expected to become an attractive and convenient real-time spectroscopic tool. The use of the mode-filtering technique enables us to utilize fully stabilized low-repetition-rate combs and tailor the feasible parameters of dual-comb spectroscopy for any application on demand, such as the measurement speed and sampling resolution. The repetition rate multiplication implies decrease in a spectral sampling resolution, but it is still useful for various application which does not require ultrahigh frequency resolution, especially since it can add other advantages such as increase in detection speed and observable spectrum bandwidth [4–8]. It is worth mentioning that the ultimate frequency resolution is determined by the mode linewidth, thus it can be better than the mode-spacing with the f_{rep} scanning [2,20].

The SNR of the filtered dual-comb was limited by the RIN caused by mode-filtering. When we use high-repetition-rate combs without mode-filtering, the RIN of the combs will limit the SNRs. This fact indicates that it is important to make lasers with a low RIN in the development of light sources for high-speed and high-sensitivity dual-comb applications.

Funding

Japan Science and Technology Agency (JST) through the ERATO MINOSHIMA Intelligent Optical Synthesizer (IOS) Project (JPMJER1304); Grant-in-Aid for JSPS Fellows (16J02345).

Acknowledgments

We thank Yutaka Iwamoto for building the Fabry–Perot cavity systems, and Eiji Tokunaga, Kazuaki Nakata, Naoyuki Shiokawa, and Masayuki Sirakawa (Tokyo University of Science) as well as Akifumi Asahara and Ken'ichi Kondo (UEC) for their assistance in the early stages of developing the Er-doped fiber lasers. We also thank Hajime Inaba and Sho Okubo (AIST) for their valuable advice concerning the dual-comb system setup, and Masaaki Hirano, Yoshinori Yamamoto, and Takemi Hasegawa of Sumitomo Electronics Inc. for providing us with highly nonlinear fibers.